Available online at www.sciencedirect.com

SciVerse ScienceDirect

Ceramics International 39 (2013) 7475–7481

CERAMICS INTERNATIONAL

www.elsevier.com/locate/ceramint

Oxidation behavior and ablation properties of MDF-based biomorphic SiC composites

Dongju Lee[a], Yun C. Kim[b], Malik Adeel Umer[a], Kwang H. Lim[c], Sang B. Park[d], Soon H. Hong[a,*]

[a]*Department of Materials Science and Engineering, KAIST, 291 Daehak-ro, Yuseong-Gu, Daejeon 307-701, Republic of Korea*
[b]*Agency for Defense Development, Yuseong-gu, Daejeon 305-152, Republic of Korea*
[c]*Daeyang Ind.,Co., Icheon-city, Gyeonggi-do 467-813, Republic of Korea*
[d]*Korea Forest Research Institute, Dongdaemun-gu, Seoul 130-712, Republic of Korea*

Received 1 December 2012; received in revised form 12 February 2013; accepted 27 February 2013
Available online 7 March 2013

Abstract

Biomorphic SiC composites were fabricated by infiltration of liquid Si into a preform fabricated from medium-density fiberboard (MDF). The phase compositions, microstructures, oxidation behaviors, and ablation properties of the composites were investigated. The composites were oxidized at elevated temperatures (up to 1450 °C) in air to study their oxidation behavior. Pores and cracks initially formed from the oxidation of residual carbon, followed by melting of residual Si. The ablation resistance of a composite was gauged using an oxy-acetylene torch. The formation of a SiO_2 layer by the oxy-acetylene flame improved the ablation resistance because molten SiO_2 spread over the ablated surface and partially sealed the pores, thus acting as an effective barrier against the inward diffusion of oxygen.

Keywords: Biomorphic; SiC composites; Oxidation behavior; Ablation; Microstructure

1. Introduction

SiC composites are promising candidate materials for thermal protection systems for jet-vanes, leading-edges, and nose-tips of reusable space vehicles, advanced aero-engines, and hypersonic transport because of their high specific strengths, thermal shock resistances, ablation resistances, and oxidation resistances at high temperatures [1,2]. These composites are mainly made by hot pressing, polymer pyrolysis, reaction bonding, reaction forming (liquid-Si infiltration), and chemical vapor infiltration [3–8]. The reaction bonding process involves pressureless infiltration of molten Si into compacted mixtures of SiC and carbon. Free carbon reacts with molten Si to form secondary SiC grains that precipitate on the original SiC particles [5]. Compared with the reaction bonding process, reaction forming has the advantage of being capable of fabricating complex and near-net shapes. This process for producing SiC requires the preparation of a porous carbon preform followed by reactive infiltration of the preform with molten Si or silicon–refractory metal (i.e., molybdenum, niobium) alloys. The resulting SiC ceramic is called a reaction-formed SiC [6,7].

Natural wood-derived biomorphic SiC composites are of interest for environmental and economic reasons [9,10]. These composites are made by pyrolysis of natural wood precursors, followed by infiltration of molten Si to form SiC phases. This process retains the initial wood structure. Biomorphic SiC composites have several advantages over traditional SiC composites. They require less energy to manufacture because of their low fabrication temperatures. A wide variety of microstructures can be obtained, which are determined by the morphology of the template biomaterials [11]. Because of their ease of formation and environmental, economic, and performance advantages, biomorphic SiC composites should be ideal candidates for high-temperature materials. To date, a number of natural

*Corresponding author. Tel.: +82 42 350 3327; fax: +82 42 350 3310.
E-mail address: shhong@kaist.ac.kr (S.H. Hong).

0272-8842/$ - see front matter © 2013 Elsevier Ltd and Techna Group S.r.l. All rights reserved.
http://dx.doi.org/10.1016/j.ceramint.2013.02.096

plants have been used as carbon preforms, including maple, bamboo, oak, and pine [12,13]. However, the properties of biomorphic SiC composites strongly depend on their pore structures, i.e., their pore sizes, pore size distributions, pore interconnectivities, and pore orientations. The properties of these composites are quite variable because of the highly anisotropic cellular structure of wood. Recently, biomorphic SiC composites having isotropic pore structures have been prepared using cellulose fiber preforms (artificial fiberboard, fiber felts, and paper) [14–16]. Cellulose fiber preforms can be used to fabricate homogeneous high-density preforms.

Research on the oxidation behavior and ablation properties of biomorphic composites has recently attracted considerable attention [17–21]. However, the oxidation behavior and ablation mechanisms warrant further study. Herein, biomorphic SiC composites were prepared by the infiltration of molten Si into carbon preforms made from medium-density fiberboard (MDF). During the process, the microstructures of the starting woods, the carbon preforms, and the composites were analyzed. Additionally, the effect of residual Si on the oxidation behavior of the MDF-based biomorphic SiC composites was investigated. The ablation properties of these composites were also studied.

2. Experimental procedure

2.1. Materials and fabrication process

Commercial MDF was used to prepare the biomorphic SiC composites. MDF is an artificial wood product created by mixing powdered wood with binders and then forming the board at high pressure and temperature. The MDF used as the precursor had a density of 0.6–0.8 g/cm^3. MDF specimens (100 mm × 100 mm × 10 mm) were dried at 100 °C for 24 h in a vacuum oven. The dried wood specimens were converted into carbon preforms by pyrolysis at 1000 °C in an atmosphere of flowing nitrogen. A carbon preform prepared by pyrolysis of MDF had a more homogeneous structure than one obtained by pyrolysis of natural wood, which has open-channel pores along the tree-growth direction.

Molten Si was infiltrated into the carbon preforms in a graphite furnace under vacuum at 1560 °C over 40 min. To produce full-density biomorphic SiC composites, an excess of the stoichiometric amount of Si was necessary (234 wt% is the quantity of Si needed to totally transform a carbon preform into SiC according to the equation Si (28.085 g/mol)+ C (12.011 g/mol)→SiC). Therefore, the weight ratio of the starting silicon to the carbon preform (W_{Si}/W_C) was set at 4:1. After the Si infiltration process, the specimens were machined so that their oxidation behaviors and ablation properties could be studied. Details of the fabrication procedures were described previously [22].

2.2. Characterization

The microstructures of the carbon preforms and the composites were examined by optical microscopy (OM, Leica DC-200), scanning electron microscopy (SEM, Philips XL30SFEG), and transmission electron microscopy (TEM, JEOL JEM-ARM200F). The pore size distribution and porosity of carbon preform were estimated using a porosimeter (Micromeritic-s, Autopore-IV 9520). The phases of the composites were characterized by X-ray diffraction (XRD, Rigaku D/Max-IIIC). The relative amounts of the different phases were estimated using the reference intensity ratio (RIR) method using RIGAKU Jade 9 program. The bulk densities of the preforms and composites were measured by the Archimedes method (ASTM 373-88). The composition of the composites was analyzed using an image analysis program (Matrox Inspector 2.1). The oxidation behaviors of the composites were determined in dry air up to 1450 °C with a thermogravimetric–differential thermal analysis (TG–DTA) instrument (Setaram 92-18) at a flow rate of 50 mL/min and a heating rate of 10 °C/min. Pulverized samples were used. Ablation tests were carried out with an oxy-acetylene torch. The diameter of the nozzle tip was 2 mm, and the distance from the nozzle tip to the specimen was 20 mm. The flow rates of the oxygen and acetylene gases were 12 L/min and 10 L/min, with pressures of 5 bar and 1.5 bar, respectively. A 10-mm-diameter specimen was exposed to the flame for 60 s. The mass and linear ablation rates were calculated from the changes in weight and thickness. The temperature of the ablated surface was measured with an infrared thermometer.

3. Results and discussion

3.1. Fabrication of the SiC composites

Wood specimens were pyrolyzed at 1000 °C under flowing nitrogen gas. Although shrinkage occurred during the pyrolysis process, the MDF carbon preforms retained their original shapes. The characteristics of the MDF samples and the carbon preforms are summarized in Table 1. Despite the high weight loss and shrinkage of the wood during the high-temperature pyrolysis process, the microstructural details of the initial wood structure were transformed with high precision into the carbon preform (Fig. 1(a) and (b)). The pore size of the MDF was generally smaller than 10 μm, and the open porosity of the carbon preforms was utilized for the Si infiltration after pyrolysis (Fig. 1(c)).

After the Si infiltration, the carbon preforms were converted into SiC. The preforms retained their original random structures. Fig. 1(d) shows the surface of the biomorphic SiC composites made from the MDF carbon preform, where the gray area is SiC, the white area is residual Si, the dark gray area is residual carbon, and the

Table 1
Microstructural characteristics of the wood, the carbon preforms, and the biomorphic composites.

Woods	Preform					Composites					
Density (g/cm^3)	Density (g/cm^3)	Porosity (%)	Pyrolysis shrinkage (%)			SiC (vol%) (wt%)	Si (vol%) (wt%)	C (vol%) (wt%)	Bulk density (g/cm^3)	Theoretical density (g/cm^3)	Relative Density (%)
			Axial	Radial	Tangential						
0.80	0.71	42.65	24.8	24.0	45.8	80.7 (87.8)	13.2 (10.4)	2.5 (1.8)	2.94	2.98	98.5

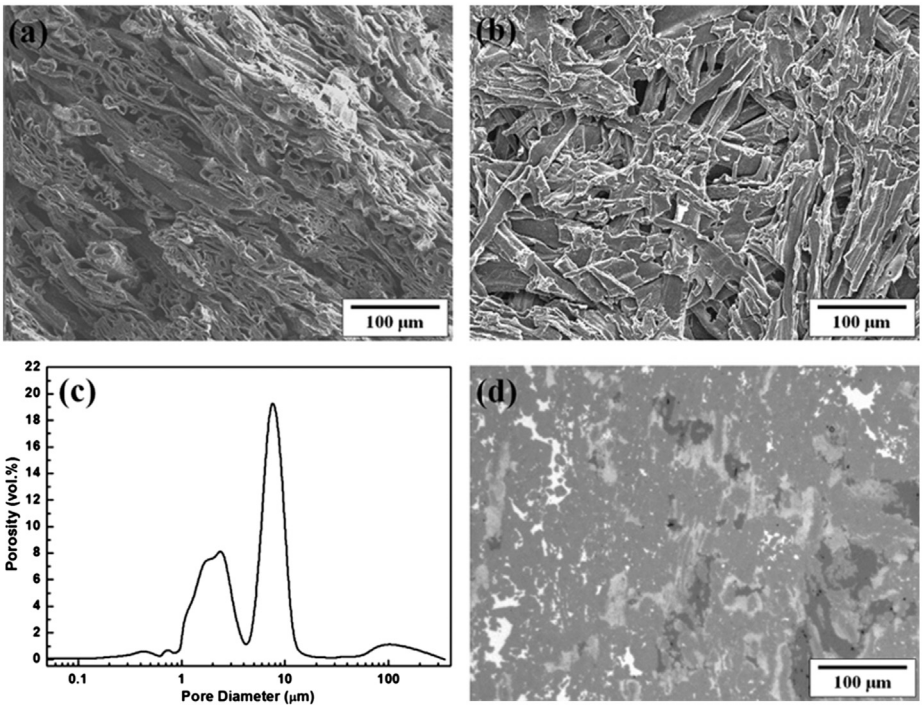

Fig. 1. SEM micrographs showing a carbon preform made from MDF (a) parallel to the pressing direction and (b) perpendicular to the pressing direction. (c) Pore size distribution of carbon preform. (d) Microstructures of the biomorphic SiC composites.

black area indicates pores. Table 1 shows the compositions, porosities, and densities of the composites.

3.2. Oxidation behavior

The oxidation behavior of the MDF-based biomorphic SiC composites was investigated with a TG–DTA instrument in flowing air. Fig. 2 shows that weight loss and an exothermic reaction started at around 500 °C and were completed at around 800 °C. A weight loss of 2.5 wt% was measured. These events occurred due to oxidation of the residual carbon into carbon monoxide and carbon dioxide:

$$C + O_2 \rightarrow CO_2 \quad (1)$$

$$2C + O_2 \rightarrow CO_2 \quad (2)$$

Above 900 °C, the TG curve showed a gradual weight gain up to about 1400 °C because of the formation of a silica layer during the oxidation of the SiC structure according to the following equations [22,23]:

$$SiC + 2O_2 \rightarrow SiO_2 + CO_2 \quad (3)$$

$$SiC + (3/2)O_2 \rightarrow SiO_2 + CO \quad (4)$$

The exothermic melting of the residual Si phase occurred at 1418 °C.

To observe the surface morphology and phase changes during oxidation at elevated temperatures, the MDF-based biomorphic composite samples were oxidized by heat treatment at 500–1500 °C in air for 1 h. Fig. 3(a) shows the XRD results. At 1500 °C, the Si peaks almost disappeared because the residual Si phases had nearly completely melted. No silica peaks were seen in the XRD results because only a small amount of silica was present. The RIR method and image analysis were applied to the XRD peaks to quantitatively estimate the SiC and residual Si contents. The amounts of these phases were comparable before oxidation (Table 1 and Fig. 3(b)). The amount of the residual Si of the biomorphic SiC samples gradually

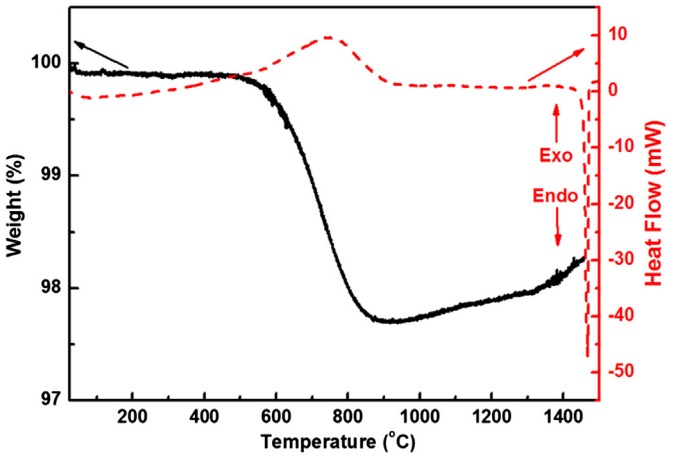

Fig. 2. (a) TGA (black solid lines) and DTA curves (red dashed lines) of the MDF-based biomorphic SiC composites. (For interpretation of the references to color in this figure legend, the reader is referred to the web version of this article.)

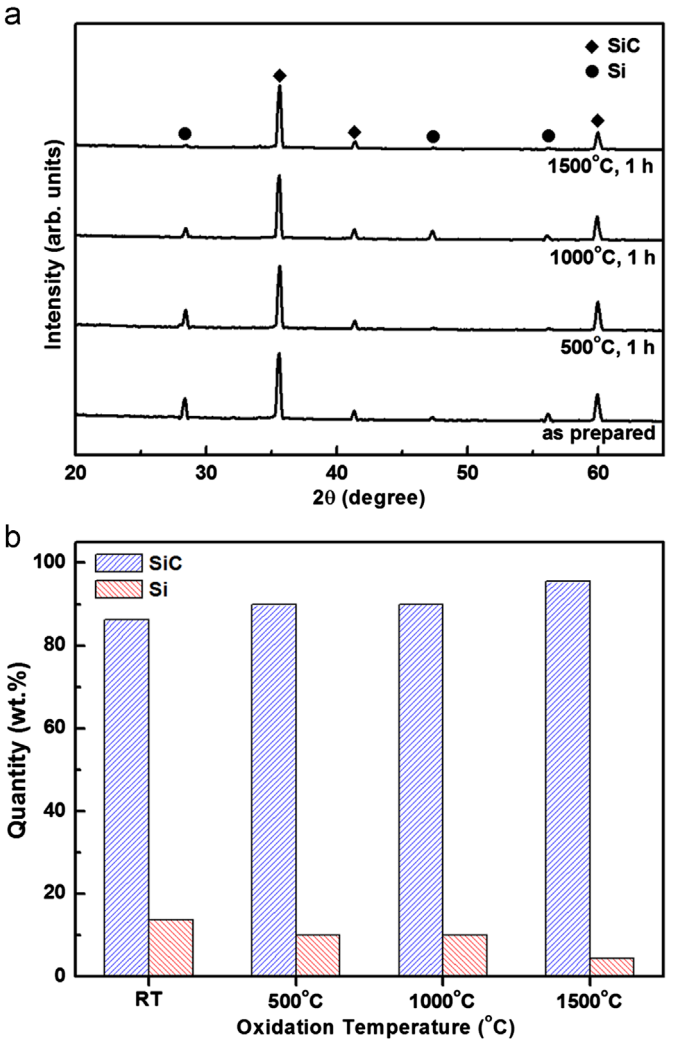

Fig. 3. (a) XRD spectra of MDF-based biomorphic SiC composites oxidized for 1 h at various temperatures. (b) Quantitative estimation of phase contents.

decreased with increasing oxidation temperature; the SiC phase dominated above the Si melting temperature (Fig. 3(b)).

Fig. 4 shows the microstructures of the MDF-based biomorphic SiC composites after oxidation. Pores and cracks formed by oxidation of the residual carbon during the 500 °C heat treatment (Fig. 4(a)). At 1500 °C, the surface morphology changed drastically. An SEM image (Fig. 4(b)) shows numerous wire-like nanostructures (straight, curved, and randomly-oriented) with lengths of tens of microns; pores and cracks are also clearly visible.

TEM was used to further investigate the wire-like nanostructures. The low-magnification TEM micrographs of Fig. 4(c) and (d) show the general morphology of the nanostructures after oxidation of the MDF-based biomorphic SiC composites. The nanostructures shown are several tens to over 100 micrometers long and have straight or curved morphologies. The nanostructures were mostly about 50 nm in diameter. The inset of Fig. 4(d) shows the chemical composition of the nanostructures as determined by energy dispersion spectroscopy (EDS). The nanostructures were mainly composed of Si and C. Further details of the SiC nanostructures were provided by the selected area electron diffraction (SAED) pattern, as shown in the inset of Fig. 4(d). The SAED pattern recorded along the [011] zone axis indicated a single-crystal structure. The nanostructures had a single-crystalline β-phase SiC core structure and a thin amorphous oxide shell. The interconnected and continuous SiC network nanostructures originated from the three-dimensional structures of the wood. The SiC network developed through the infiltration of liquid Si along the internal channels of the carbon preform during the fabrication process, and this network was buried in carbon and residual Si before oxidation. These SiC network nanostructures were exposed by oxidation of the residual carbon and migration of liquid Si at high temperatures. Well-interconnected and continuous SiC network nanostructures play an important role in high-temperature mechanical properties by supporting loads [24]. The thin amorphous oxide shell on the SiC nanostructures was formed by oxidation of the SiC network.

3.3. Ablation behavior

The ablation behaviors of the MDF-based biomorphic SiC composites are summarized in Table 2. After ablation for 60 s, the mass and linear ablation rates were 5.7×10^{-4} g/cm^2 s and 1.2×10^{-3} mm/s, respectively. Ablation results from a combination of oxidation and erosion due to the high temperature, pressure, and velocity of the oxy-acetylene flame [25,26]. After 60 s of ablation, the surface temperature reached 2100–2200 °C, which is higher than the melting point of SiO_2 (1723 °C). The liquid SiO_2 at the ablation center was swept out by the gas flow of the high-temperature and high-speed oxy-acetylene flame, and thus the thickness of the composite decreased. As the SiO_2 melted, molten SiO_2 spread over the ablated surface,

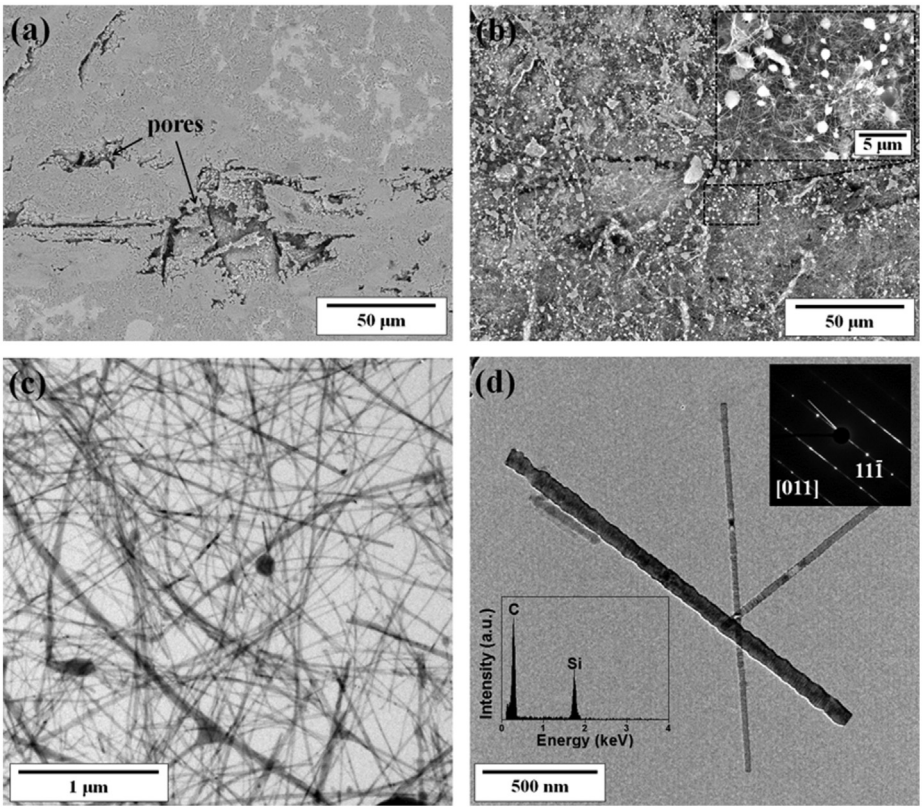

Fig. 4. SEM images of MDF-based biomorphic SiC composites oxidized for 1 h at (a) 500 °C and (b) 1500 °C. (c) Low-magnification TEM micrographs of wire-like nanostructures after oxidation at 1500 °C for 1 h. (d) EDS results and SAED pattern along the [011] zone axis, revealing an SiC single-crystal nanostructure.

Table 2
Ablation properties of the MDF-based biomorphic SiC composites.

Ablation time	**60 s**
Surface temperature	**2100–2200 °C**
Mass change	**1.546 g → 1.519 g**
Thickness change	**3.014 mm → 2.942 mm**
Mass ablation rate	**5.7×10^{-4} g/cm^2 s**
Linear ablation rate	**1.2×10^{-3} mm/s**

partially sealed the pores, and acted as an effective barrier against inward diffusion of oxygen [27].

Fig. 5 shows SEM and OM micrographs of the as-ablated MDF-based biomorphic SiC composites. After ablation for 60 s, a white and dense scale was observed on the surface by OM examination (Fig. 5(a)); it was oxidized SiO_2. Fig. 5(b) and (d) are cross-sectional OM and SEM images of the center region. The thickness of the oxidized region was about 300 μm. Another SEM image (Fig. 5(c)) shows that some microholes and bubble-shaped pits were present in the SiO_2 layer. Oxidation of the SiC coating resulted in the escape of CO and CO_2 gases, which formed these defects [28]. The formation of the SiO_2 layer helped to improve the ablation resistance because it acted as a thermal barrier as well as reduced the diffusion of oxygen.

XRD was also used to study the ablated MDF-based biomorphic SiC composites (Fig. 6). Si, β-SiC, and α-SiC were identified. The surface XRD pattern of a sample after the ablation test showed a less intense Si peak than before the test. This indicated that the residual Si and SiC phases of the composites were oxidized during the ablation test to form a smooth outer SiO_2 glass layer. SiO_2 phases were not detected by XRD because the oxidized SiO_2 layer was a glassy phase and not crystalline. Peaks for the α-SiC phase were detected after ablation because the phase transition from β-SiC to α-SiC occurred when the oxy-acetylene flame temperature exceeded 1700 °C [29].

4. Conclusions

MDF-based biomorphic SiC composites were fabricated by infiltration of liquid Si into pyrolyzed carbon MDF preforms. These composites were oxidized at elevated temperatures. Pores and cracks were formed from the oxidation of residual carbon. In oxy-acetylene torch testing, the mass and linear ablation rates of the composite were 5.7×10^{-4} g/cm^2 s and 1.2×10^{-3} mm/s respectively. Liquid SiO_2 formed by the oxy-acetylene flame was swept away by the flushing action of the high-temperature and high-speed gas flow and spread over the ablation surface, partially sealing the pores. The formation of an SiO_2 layer helped to improve the ablation resistance because it acted as a thermal barrier as well as reduced the diffusion of oxygen.

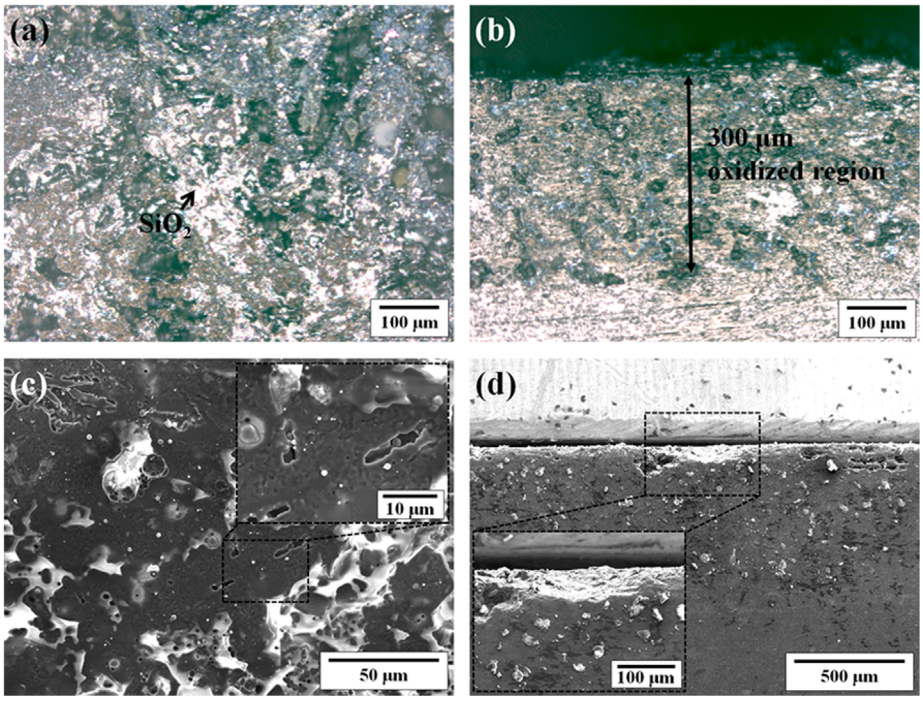

Fig. 5. OM and SEM images of the MDF-based biomorphic SiC composites after the oxy-acetylene torch test: (a) and (c) surface, (b) and (d) cross-section. The inset is a higher-magnification SEM image.

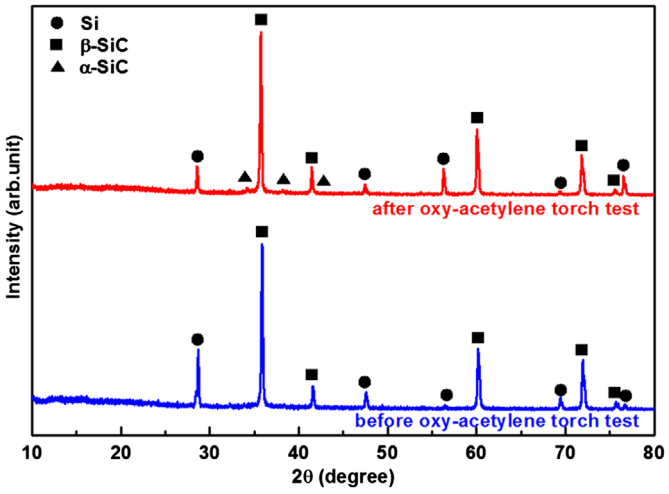

Fig. 6. XRD patterns of specimen surfaces before and after the oxy-acetylene torch testing of the MDF-based biomorphic SiC composites.

Acknowledgment

This research was supported by the Defense Acquisition Program and the Agency for Defense Development under Contract UD070033AD and by NSL (National Space Lab.) program through the Korea Science and Engineering Foundation funded by the Ministry of Education, Science and Technology (2008-2003213) and by Priority Research Centers Program through the National Research Foundation of Korea (NRF) funded by the Ministry of Education, Science and Technology (2011-0031407).

References

[1] S. Kumar, A. Kumar, K. Sampath, V.V.B. Prasad, J.C. Chaudhary, A.K. Gupta, G.R. Devi, Fabrication and erosion studies of C–SiC composite Jet Vanes in solid rocket motor exhaust, Journal of the European Ceramic Society 31 (2011) 2425–2431.

[2] T. Ogasawara, T. Aoki, M.S.A. Hassan, Y. Mizokami, N. Watanabe, Ablation behavior of SiC fiber/carbon matrix composites under simulated atmospheric reentry conditions, Composites Part A 42 (2011) 221–228.

[3] O.P. Chakrabarti, S. Ghosh, J. Mukerji, Influence of grain-size, free silicon content and temperature on the strength and toughness of reaction-bonded silicon-carbide, Ceramics International 20 (1994) 283–286.

[4] P. Greil, Near net shape manufacturing of polymer derived ceramics, Journal of the European Ceramic Society 18 (1998) 1905–1914.

[5] S. Aroati, M. Cafri, H. Dilman, M.P. Dariel, N. Frage, Preparation of reaction bonded silicon carbide (RBSC) using boron carbide as an alternative source of carbon, Journal of the European Ceramic Society 31 (2011) 841–845.

[6] M. Singh, R.M. Dickerson, SiC (SCS-6) fiber reinforced–reaction formed SiC matrixcomposites: microstructure and interfacial properties, Journal of Materials Research 12 (1997) 706–713.

[7] S. Xu, G. Qiao, D. Li, H. Yang, Y. Liu, T. Lu, Reaction forming of silicon carbide ceramic using phenolic resin derived porous carbon preform, Journal of the European Ceramic Society 29 (2009) 2395–2402.

[8] E. Vogli, H. Sieber, P. Greil, Biomorphic SiC-ceramic prepared by Si-vapor phase infiltration of wood, Journal of the European Ceramic Society 22 (2002) 2663–2668.

[9] G.L. Liu, P.Y. Dai, Y.Z. Wang, J.F. Yang, Y.B. Zhang, Fabrication of wood-like porous silicon carbide ceramics without templates, Journal of the European Ceramic Society 31 (2011) 847–854.

[10] D. Mallick, O.P. Chakrabarti, H.S. Maiti, R. Majumdar, Si/SiC ceramics from wood of Indian dicotyledonous mango tree, Ceramics International 33 (2007) 1217–1222.

[11] M. Singh, B.M. Yee, Reactive processing of environmentally conscious, biomorphic ceramics from natural wood precursors, Journal of the European Ceramic Society 24 (2004) 209–217.
[12] H.S. Park, J.J. Jang, K.H. Lee, K.H. Lim, S.B. Park, Y.C. Kim, S.H. Hong, Effects of microstructure on flexural strength of biomorphic C/SiC composites, International Journal of Fracture 151 (2008) 233–245.
[13] J.T. Zhu, F.L. Kwong, D.H.L. Ng, Synthesis of biomorphic SiC ceramic from bamboo charcoal, Journal of Nanoscience and Nanotechnology 9 (2009) 1564–1567.
[14] G. Amirthan, A. Udayakumar, V.V.B. Prasad, M. Balasubramanian, Solid particle erosion studies on biomorphic Si/SiC ceramic composites, Wear 268 (2010) 145–152.
[15] T.S. Orlova, V.V. Popov, J.Q. Cancapa, D.H. Maldonado, E.E. Magarino, F.M.V. Feria, A.R. de Arellano, J.M. Fernandez, Electrical properties of biomorphic SiC ceramics and SiC/Si composites fabricated from medium density fiberboard, Journal of the European Ceramic Society 31 (2011) 1317–1323.
[16] M.A. Bautista, A.R. de Arellano-Lopez, J. Martinez-Fernandez, A. Bravo-Leon, J.M. Lopez-Cepero, International Journal of Refractory Metals and Hard Materials 27 (2009) 431–437.
[17] H. Ghanem, E. Alkhateeb, H. Gerhard, N. Popovska, Oxidation behavior of silicon carbide based biomorphic ceramics prepared by chemical vapor infiltration and reaction technique, Ceramics International 38 (2009) 2767–2774.
[18] H. Ghanem, H. Gerhard, N. Popovska, Paper derived SiC–Si_3N_4 ceramics for high temperature applications, Ceramics International 35 (2009) 1021–1026.
[19] G. Amirthan, A. Udayakumar, V.V.B. Prasad, M. Balasubramanian, Properties of Si/SiC ceramic composite subjected to chemical vapour infiltration, Ceramics International 35 (2009) 2601–2607.
[20] W. Gong, P. Gao, W. Wang, Characterization and oxidation properties of biomorphic porous carbon with SiC gradient coating prepared by PIP method, Ceramics International 37 (2011) 1739–1746.
[21] A. Maity, D. Kalita, N. Kayal, T. Goswami, O. Chakrabarti, P.G. Rao, Oxidation behavior of SiC ceramics synthesized from processed cellulosic bio-precursor, Ceramics International 38 (2012) 4701–4706.
[22] D.J. Lee, J.J. Jang, H.S. Park, Y.C. Kim, K.H. Lim, S.B. Park, S.H. Hong, Fabrication of biomorphic SiC composites using wood preforms with different structures, Ceramics International 38 (2012) 3089–3095.
[23] F. Lamouroux, R. Naslain, J.M. Jouin, Kinetics and mechanisms of oxidation of 2d woven C/SiC composites 2. Theoretical approach, Journal of the American Ceramic Society 77 (1994) 2058–2068.
[24] M. Presas, J.Y. Pastor, J. LLorca, A.R. de Arellano-Lopez, J. Martínez-Fernandez, R.E. Sepulveda, Mechanical behavior of biomorphic Si/SiC porous composites, Scripta Materialia 53 (2005) 1175–1180.
[25] D. Fang, Z.F. Chen, Y.D. Song, Z.G. Sun, Morphology and microstructure of 2.5 dimension C/SiC composites ablated by oxyacetylene torch, Ceramics International 35 (2009) 1249–1253.
[26] W. Yong-Jie, L. He-Jun, F. Qian-Gang, W. Heng, Y. Dong-Jia, W. Bing-Bo, Ablative property of HfC-based multilayer coating for C/C composites under oxy-acetylene torch, Applied Surface Science 257 (2011) 4760–4763.
[27] D. Zhao, C.R. Zhang, H.F. Hu, Y.D. Zhang, Ablation behavior and mechanism of 3D C/ZrC composite in oxyacetylene torch environment, Composites Science and Technology 71 (2011) 1392–1396.
[28] J.F. Huang, M. Liu, B. Wang, L.Y. Cao, C.K. Xia, J.P. Wu, SiC_n/SiC oxidation protective coating for carbon/carbon composites, Carbon 47 (2009) 1198–1201.
[29] P. Krishna, R.C. Marshall, Structure, perfection and annealing behaviour of SiC needles grown by a VLS mechanism, Journal of Crystal Growth 9 (1971) 319–325.